Nephrol Dial Transplant (2000) 15 [Suppl 6]: 23–25

Nephrology
Dialysis
Transplantation

Structural analyses of the aquaporin super-family

A. Engel

M. E. Müller-Institute for Microscopy at the Biozentrum, University of Basel, CH-4056 Basel, Switzerland

Key words: aquaporins; electron crystallography; electron microscopy

Introduction

Water passes through biological membranes by two different mechanisms: either by diffusion through pure lipid bilayers (activation energy $E_a > 10$ kcal/mol) or through specific pores, the aquaporins ($E_a < 5$kcal/mol). The permeation of this pore is remarkably specific, since other small molecules, ions or even protons (H_3O^+) are not accommodated. An abundant 28 kDa protein with homology to the putative channel protein MIP (now also termed AQP0) of lens fibre cells [1], was discovered in red cell membranes [2]. This protein was identified as a water channel by expressing it in *Xenopus laevis* oocytes, and measuring water permeation [3]. It is now known as aquaporin 1 (AQP1).

Many proteins related to AQP1 and AQP0 have been found subsequently in diverse life forms [4]. The aquaporin super-family includes strict water channels as well as channels transporting solutes such as urea and glycerol. Importantly, a channel allowing the passage of water but blocking the passage of ions should not dissipate the transmembrane potential. Therefore, aquaporins must contain specific sites that prevent ions from passing through the channel.

Aquaporins are tetrameric proteins that assemble into 2D arrays

AQP1 is a square-shaped homotetramer of ~70 Å size containing four independent aqueous channels [5–8]. Similarly, AQP0 solubilized in decylmaltoside has a mass of 160 kDa and exhibits a size of 70 Å [9]. The *Escherichia coli* water channel, AqpZ, is a square-shaped particle after solubilization in octylglucoside and negative staining [10]. The solubilized bacterial glycerol facilitator GlpF is a square-shaped particle of 90–100 Å side length, also suggesting a tetrameric protein [11]. However, the requirement for tetramerization of a protein that forms four apparently independent channels remains a puzzle.

When reconstituted into lipid bilayers, AQP1 forms two-dimensional (2D) lattices with a unit cell of 96 Å side length containing two tetramers in opposite orientation [12,13]. AqpZ crystallizes in a similar manner [10], while AQP0 assembles into tetragonal arrays with a single tetramer per unit cell of 64 Å side length [9,14]. GlpF shows yet another packing arrangement, with unit cells of 104 Å side length housing two tetramers packed in opposite orientation, but exhibiting a p4 symmetry [11]. Projection maps obtained from these lattices by cryo-electron microscopy revealed quite similar features. The common motif includes four monomers comprising a low-density region surrounded by 7–9 density maxima, depending on the resolution achieved (Figure 1). The density minimum within monomers is always shifted towards the 4-fold centre, where the lowest density within the tetramer is found. Monomers are separated by gaps arranged in a cross, which exhibit pronounced low-density regions in AQP1 and AqpZ. Clearly, GlpF possesses the most prominent low density region which is most probably the pore [11].

The 3D structure of AQP1

The three-dimensional (3D) structure of AQP1 has been determined at 6 Å resolution by cryo-electron microscopy. Each AQP1 monomer has six tilted, bilayer-spanning α-helices [15] that form a right-handed bundle surrounding a central density [8,16]. At 4.5 Å resolution, several rod-shaped densities reveal protrusions that follow a right-handed helical pattern consistent with the expected density of an α-helix [17].

Site-directed mutagenesis on the loops containing NPA motifs leads to the 'hourglass' model in which an intracellular NPA loop and an extracellular NPA loop project back into the membrane bilayer where their intersection forms a narrow aperture [5]. This prediction was confirmed by the shape of the central

Correspondence and offprint requests to: A. Engel, M. E. Müller Institute for Microscopy at the Biozentrum, University of Basel, CH-4056 Basel, Switzerland.

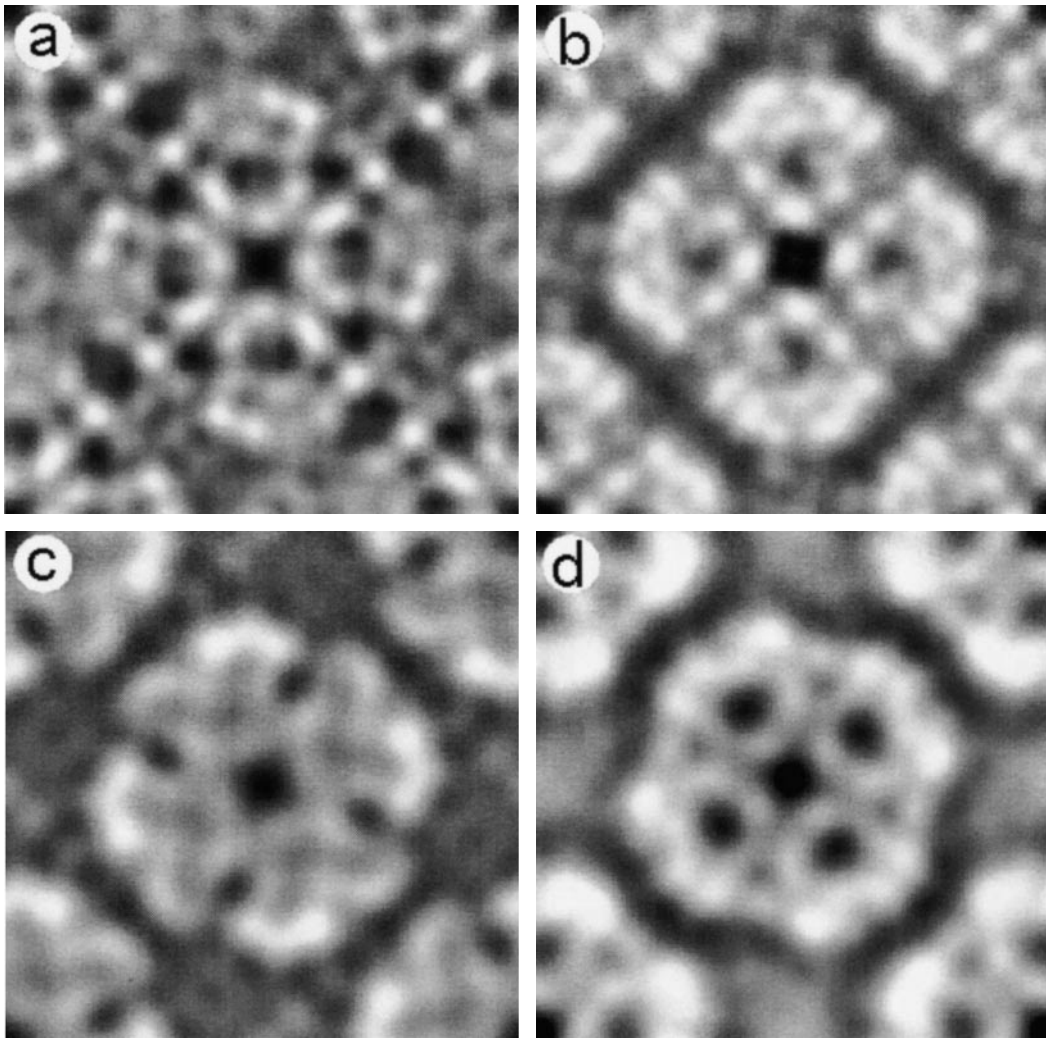

Fig. 1. Projection maps of water channel proteins acquired by cryo-electron microscopy. (**a**) The red cell water channel, AQP1, at 3.5 Å resolution. AQP1 packs into arrays with $P42_12$ symmetry, housing two tetramers per unit cell of size 96 Å. (**b**) The lens fibre cell water channel, AQP0, at 5.7 Å resolution [14]. AQP0 packs into P4 arrays with a single tetramer per unit cell of 64 Å side length. The area shown comprises two unit cells. (**c**) The bacterial water channel, AqpZ, at 8 Å resolution [10]. AqpZ is packed in an up-and-down orientation as AQP1 into unit cells of 94 Å width. (**d**) The bacterial glycerol diffusion facilitator, GlpF, rendered here at 7 Å resolution [11]. Two GlpF tetramers are packed in an up-and-down orientation into unit cells of 104 Å width, but the crystals exhibit a P4 symmetry. All projections are viewed from the cytoplasmic side.

density, which consists of two V-shaped regions touching one another in the centre of the AQP1 monomer to form the density 'X' [8]. At 4.5 Å resolution, the central density is now resolved as two short helices projecting outwards from the centre of the monomer, connected to adjacent helices by loop regions [17].

Major differences between AQPs and GLPs

The similarity of projection maps (Figure 1) suggests that the architecture of these proteins, namely AQP1, AQP0, AqpZ and GlpF, is similar within the membrane core which houses the six helices and two functional loops. The major difference between AQPs and GLPs is that loop E is longer by $\sim$10–15 residues in the latter, but this difference still needs to be visualized and its functional implication to be unravelled. Froger *et al.* [18] have proposed to distinguish the AQPs and the GLPs based on five particular amino acid residues. Further clues are found in the more recent sequence analysis by Heymann and Engel [19], who have identified two critical conserved hydrophobic residues in the middle of helices 1 and 4.

Perspectives

The atomic structures of members of the two subfamilies AQP and GLP of the aquaporin super-family are now required in order to understand the function of these ubiquitous channels. Such knowledge is important, since it ultimately may be used to develop therapeutic agents for important clinical disorders. 3D

maps from electron crystallographic analyses now approach a sufficient resolution to build an atomic model, and highly ordered 2D crystals of AQP0, AQP1, AqpZ, α-TIP [20] and GlpF [11] are now available. This progress promises that this goal should be reached soon.

References

1. Gorin MB, Yancey SB, Cline J, Revel J-P, Horwitz J. The major intrinsic protein (MIP) of the bovine lens fiber membrane: characterization and structure based on cDNA cloning. *Cell* 1984; 39: 49–59
2. Preston GM, Agre P. Isolation of the cDNA for erythrocyte integral membrane protein of 28 kilodaltons: member of an ancient channel family. *Proc Natl Acad Sci USA* 1991; 88: 11110–11114
3. Preston GM, Carroll TP, Guggino WB, Agre P. Appearance of water channels in *Xenopus* oocytes expressing red cell CHIP28 protein. *Science* 1992; 256: 385–387
4. Heymann J, Engel A. Aquaporins: phylogeny, structure and physiology of water channels. *News Physiol Sci* 1999; 14: 187–193
5. Jung J, Preston G, Smith B, Guggino W, Agre P. Molecular structure of the water channel through aquaporin CHIP. The hourglass model. *J Biol Chem* 1994; 269: 14648–14654
6. Smith BL, Agre P. Erythrocyte M_r 28,000 transmembrane protein exists as a multisubunit oligomer similar to channel proteins. *J Biol Chem* 1991; 266: 6407–6415
7. Verbavatz J-M, Brown D, Sabolic I *et al.* Tetrameric assembly of CHIP28 water channels in liposomes and cell membranes: a freeze-fracture study. *J Cell Biol* 1993; 123: 605–618
8. Walz T, Hirai T, Murata K *et al.* The 6 Å three-dimensional structure of aquaporin-1. *Nature* 1997; 387: 624–627
9. Hasler L, Walz T, Tittmann P, Gross H, Kistler J, Engel A. Purified lens major intrinsic protein (MIP) forms highly ordered tetragonal two-dimensional arrays by reconstitution. *J Mol Biol* 1998; 279: 855–864
10. Ringler P, Borgnia MJ, Stahlberg H, Agre P, Engel A. Structure of the water channel AqpZ from *Escherichia coli* revealed by electron crystallography. *J Mol Biol* 1999; 291: 1181–1190
11. Braun T, Philippsen A, Wirtz S *et al.* Projection structure of the glycerol facilitator at 3.5 Å resolution. *EMBO Rep* 2000; 1: 183–189
12. Jap BK, Li H. Structure of the osmo-regulated H_2O-channel, AQP-CHIP, in projection at 3.5 Å resolution. *J Mol Biol* 1995; 251: 413–420
13. Walz T, Smith B, Agre P, Engel A. The three-dimensional structure of human erythrocyte aquaporin CHIP. *EMBO J* 1994; 13: 2985–2993
14. Fotiadis D, Hasler L, Müller DJ, Stahlberg H, Kistler J, Engel A. The surface topography of lens MIP supports dual functions. *J Mol Biol* 2000; 300: 779–789
15. Li H, Lee S, Jap BK. Molecular design of aquaporin-1 water channel as revealed by electron crystallography. *Nature Struct Biol* 1997; 4: 263–265
16. Cheng A, van Hoek AN, Yeager M, Verkman AS, Mitra AK. Three-dimensional organization of a human water channel. *Nature* 1997; 387: 627–630
17. Mitsuoka K, Murata K, Walz T *et al.* Short-helices in hourglass pore-forming domains of AQP1 water channel protein visualized at 4.5 Å. *J Struct Biol* 1999; 128: 34–43
18. Froger A, Tallur B, Thomas D, Delamarche C. Prediction of functional residues in water channels and related proteins. *Protein Sci* 1998; 7: 1458–1468
19. Heymann JB, Engel A. Structural clues in the sequences of the aquaporins. *J Mol Biol* 2000; 295: 1039–1053
20. Daniels MJ, Chrispeels MJ, Yeager M. 2D crystallization of a plant vacuole membrane aquaporin and determination of its projection structure by electron crystallography. *J Mol Biol* 1999; 294: 1337–1349